MECHANISMS OF SIGNAL TRANSDUCTION:

TUCAN, an Antiapoptotic Caspase-associated Recruitment Domain Family Protein Overexpressed in Cancer

Nuzhat Pathan, Hiroyuki Marusawa, Maryla Krajewska, Shu-ichi Matsuzawa, Hoguen Kim, Kazuya Okada, Seiji Torii, Shinichi Kitada, Stanislaw Krajewski, Kate Welsh, Frederick Pio, Adam Godzik and John C. Reed

J. Biol. Chem. 2001, 276:32220-32229.
doi: 10.1074/jbc.M100433200 originally published online June 14, 2001

THE JOURNAL OF BIOLOGICAL CHEMISTRY
Vol. 276, No. 34, Issue of August 24, pp. 32220–32229, 2001
Printed in U.S.A.

TUCAN, an Antiapoptotic Caspase-associated Recruitment Domain Family Protein Overexpressed in Cancer*

Received for publication, January 17, 2001, and in revised form, June 14, 2001
Published, JBC Papers in Press, June 14, 2001, DOI 10.1074/jbc.M100433200

Nuzhat Pathan‡§, Hiroyuki Marusawa§, Maryla Krajewska, Shu-ichi Matsuzawa, Hoguen Kim‖, Kazuya Okada, Seiji Torii, Shinichi Kitada, Stanislaw Krajewski, Kate Welsh, Frederick Pio¶, Adam Godzik, and John C. Reed‡‡**

From the Burnham Institute, La Jolla, California 92037 and the ‖Department of Pathology, College of Medicine, Yonsei University, C.P.O. Box 8044, Seoul, Korea

Caspase-associated recruitment domains (CARDs) are protein interaction domains that participate in activation or suppression of CARD-carrying members of the caspase family of apoptosis-inducing proteases. A novel CARD-containing protein was identified that is overexpressed in some types of cancer and that binds and suppresses activation of procaspase-9, which we term TUCAN (tumor-upregulated CARD-containing antagonist of caspase nine). The CARD domain of TUCAN selectively binds itself and procaspase-9. TUCAN interferes with binding of Apaf1 to procaspase-9 and suppresses caspase activation induced by the Apaf1 activator, cytochrome *c*. Overexpression of TUCAN in cells by stable or transient transfection inhibits apoptosis and caspase activation induced by Apaf1/caspase-9-dependent stimuli, including Bax, VP16, and staurosporine, but not by Apaf1/caspase-9-independent stimuli, Fas and granzyme B. High levels of endogenous TUCAN protein were detected in several tumor cell lines and in colon cancer specimens, correlating with shorter patient survival. Thus, TUCAN represents a new member of the CARD family that selectively suppresses apoptosis induced via the mitochondrial pathway for caspase activation.

Apoptosis is a cell suicide process that plays important roles in multiple facets of normal development and physiology as well as many diseases (reviewed in Refs. 1 and 2). Apoptosis is caused by caspases, a family of cysteine proteases that cleave target proteins at aspartyl residues (3, 4). Caspases are initially produced as inactive zymogens, which become activated typically by proteolytic cleavage at aspartic acid residues, generating the catalytic subunits of the active enzymes. Caspases can be broadly divided into two classes: upstream initiators and downstream effectors (3, 4). The downstream caspases are thought to be activated primarily by cleavage by upstream caspases.

The proforms of initiator and effector caspases differ principally in the length of their N-terminal prodomains, the region preceding the catalytic portion of these polypeptides. Upstream initiator caspases contain large prodomains, and these domains serve as protein interaction motifs that participate in zymogen activation. A common method of activating upstream caspases involves the induced proximity mechanism, where the N-terminal prodomains are used for achieving clustering of caspase zymogens. Because uncleaved procaspases commonly display at least weak protease activity, bringing them into close apposition results in transproteolytic cleavage and activation (reviewed in Ref. 5).

The caspase-associated recruitment domain (CARD)[1] is a protein interaction motif found in the N-terminal prodomains of several caspases and in apoptosis-regulatory proteins that either activate or suppress activation of CARD-containing procaspases (6). In mammals, eight CARD-carrying caspases have been identified, including procaspase-1, -2, -4, -5, -9, -11, -12, and -13. To date, multiple noncaspase CARD-containing proteins have been discovered and functionally characterized, including Apaf1, Nod1 (CARD4), NAC (DEPCAP), Raidd (CRADD), Cardiak (Rip2, RICK), Bcl10 (CIPER), ARC (Nop30), Asc, CARD9, CARD10, CARD11, CARD14, cIAP1, cIAP2, and CLAN. The CARD domains of many of these proteins are capable of binding the CARD-containing prodomains of specific CARD-carrying caspases, either facilitating or inhibiting protease activation. Here we describe a new antiapoptotic member of the human CARD family that is overexpressed in some types of cancer and selectively binds and inhibits activation of procaspase-9.

MATERIALS AND METHODS

Computational Methods—Starting from the sequence of the CARD domain of Apaf1 (7), a cascade of PSI-BLAST (8) searches was performed, using new "hits" as queries for subsequent searches, until no new hits were found, as described elsewhere (9). Lower significance hits from this procedure ("saturated BLAST") were confirmed (or rejected) using the profile-to-profile alignment algorithm FFAS (10) against a library of apoptosis-related domains. The detailed analysis of three-dimensional models of the putative CARD domains was a final criterion in accepting/rejecting distant members of the family. After the complete list of proteins in the CARD family was assembled, representative

* This work was supported by National Institutes of Health Grants AG15402, CA69381, and NS36821; CaP-CURE; the Leukemia and Lymphoma Society of America; The National Science Foundation (NSF DB1-0078731); and the Department of Defense (DAMD17-97-1-7294). The costs of publication of this article were defrayed in part by the payment of page charges. This article must therefore be hereby marked "*advertisement*" in accordance with 18 U.S.C. Section 1734 solely to indicate this fact.

‡ Present address: IDEC Pharmaceuticals, Inc, San Diego, CA 92191.
§ These two authors contributed equally to this work.
¶ Present address: Simon Fraser University, Burnaby, British Columbia V5A 1S6, Canada.
** Present address: Dept. of Molecular Medicine, Gunma University, Gunma 371-8512, Japan.
‡‡ To whom correspondence should be addressed: The Burnham Institute, 10901 N. Torrey Pines Rd., La Jolla, CA 92037. Tel.: 858-646-3140; Fax: 858-646-3194; E-mail: jreed@burnham.org.

[1] The abbreviations used are: CARD, caspase-associated recruitment domain; TUCAN, tumor-upregulated CARD-containing antagonist of caspase nine; EST, expressed sequence tag; DAPI, 4′,6-diamidino-2-phenylindole; AFC, aminofluorocoumarin; HA, hemagglutinin; DTT, dithiothreitol; GST, glutathione *S*-transferase; IVT, in vitro translated; GraB, granzyme B; STS, staurosporine; PAGE, polyacrylamide gel electrophoresis.

members of the family were used to scan genomic and EST data bases with the TBLASTN program. Genomic regions where similarity to the CARD domain was found were again verified against the FFAS server and later analyzed with gene finding programs (9) for the presence of other domains until a complete protein sequence was assembled. Three-dimensional models of CARD domains were generated using the MODELLER program (11), based on FFAS alignments. The TUCAN cDNA sequence was found using PSI-BLAST and the CARD sequence of Nod1 as a query. This search revealed homology with a predicted protein of EST clone KIAA0955 in the KDRI brain genomic data base (available on the Internet at www.kazusa.or.jp/en/data base.html).

Plasmid Construction and cDNA Cloning—Human cDNA clones encoding the entire open reading frame of TUCAN were amplified using *Pfu* polymerase (Stratagene) using two-step polymerase chain reaction with two sets of oligonucleotide primers: set 1 (5′-GACCCTTTGTGACATCTCACA-3′ (forward) and 5′-CCAATGACAACGCTGGATTC-3′ (reverse)) and set 2 (5′- GGAATTCAAGATGATGAGACAGAGGCAG-3′ (forward) and 5′-CCCTCGAGCCAATGAGAACGCTGGATTC-3′ (reverse)). The resultant cDNA fragments were digested with *Eco*RI/*Xho*I and ligated into mammalian expression vectors pcDNA3-Myc, pcDNA3-HA, and pcDNA-3-FLAG at *Eco*RI and *Xho*I cloning sites. The nucleotide sequence of the assembled full-length TUCAN was confirmed by DNA sequencing analysis (www.sciencereagents.com). The region encoding the CARD domain was polymerase chain reaction-amplified from the cDNA using the primers 5′-GGAATTCTCAGGTGCAGCCTTTGT-3′ (forward) and 5′- CCCTCGAGCCAATGAGAACGCTGGATTC-3′ (reverse). Resulting fragments were digested with *Eco*RI/*Xho*I and ligated into pcDNA3-Myc, pcDNA3-HA, pJG4–5, pGilda, and pGEX-4T1 using *Eco*RI and *Xho*I sites. The ΔCARD construct was made using a similar strategy and the primers 5′- GGAATTCAAGATGATGAGACAGAGGCAG-3′ (forward) and 5′- AGGCTCGAGTCATGCAGCTACAAGCTGGAG-3′ (reverse).

Transfections and Cell Culture—Cells were cultured at 37 °C in 5% CO_2 in Dulbecco's modified Eagle's medium with 10% heat-inactivated fetal bovine serum, 1 mM L-glutamine, and antibiotics. For transient transfection assays, 293T cells in log phase were transfected with plasmids encoding full-length or fragments of TUCAN, procaspase-9, Apaf1, or other proteins using SuperFect transfection reagent (Qiagen). Cells were harvested 48 h later and used for immunoprecipitation and immunoblotting studies.

Jurkat cells were maintained in culture in RPMI 1640, 10% fetal bovine serum, 1 mM L-glutamine medium. For stable transfections, Jurkat cells were subjected to electroporation (2.5 kV/cm; 950 microfarads; Bio-Rad Gene Pulsar) using 10 μg of *Pvu*I-linearized pcDNA3 or 10 μg of linearized pcDNA3-Myc-TUCAN. After 2 days, cells were seeded at 10^6/ml in medium containing 1 mg/ml G418 (Omega Scientific, Inc.). Medium was replaced twice weekly, until colonies of stably transfected clones arose. Multiple clones were pooled and expanded in culture.

Apoptosis and Cell Death Assays—Cells were transfected with pEGFP (CLONTECH) and effector plasmids using SuperFect transfection reagents (Qiagen) as indicated. After 24 h, both floating and adherent cells were pooled, fixed with 3.7% formaldehyde/phosphate-buffered saline, and stained with 1 μg/ml 4′,6-diamidino-2-phenylindole (DAPI), and the percentage of green fluorescent protein-positive cells with apoptotic morphology (nuclear fragmentation, chromatin condensation) was determined by fluorescence microscopy.

Caspase Activity Measurements—Caspase activity was measured in cell lysates from HEK293T and Jurkat cells (normalized for total protein content), monitoring release of AFC from fluorogenic substrate acetyl-aspartyl-glutamyl-valinyl-aspartyl-aminofluorocoumarin (Ac-DEVD-AFC) using a spectrofluorimeter in continuous mode, as described (12). For some experiments, cytochrome *c*, dATP, or granzyme B was added as described (12).

Alternatively, cytosolic extracts from MCF7 cells were suspended in 100 μl of caspase assay buffer and incubated with 5 μl of anti-TUCAN antiserum or preimmune serum and 20 μl of protein A-Sepharose at 4 °C for 1 h. Sepharose beads were pelleted by centrifugation, and 15 μl of the resulting supernatants were supplemented with 1 μl of *in vitro* translated procaspase-3 (13), before adding either 10 μM cytochrome *c* (Sigma) and 1 mM dATP or 10 ng of granzyme B (Calbiochem), followed by 100 μM Ac-DEVD-AFC for measuring caspase activity as above.

Antibodies—Polyclonal antisera were generated in rabbits using KLH- and OVA-conjugated (Pierce) synthetic peptides with sequences corresponding to the residues 126–147 of TUCAN (Bur215) or purified recombinant GST-tagged CARD domain of TUCAN (Bur206) as immunogens. Epitope-specific antibodies for FLAG, HA, or Myc tag were obtained from Sigma, Roche Molecular Biochemicals, and Santa Cruz Biotechnology, Inc. (Santa Cruz, CA), respectively. Anti-caspase-9 antiserum (Bur49) has been described previously (14). Anti-Apaf-1 antibody was obtained from Cayman Chemical Co.

Co-immunoprecipitations and Immunoblotting Assays—For immunoprecipitation and immunoblotting analysis, cells were lysed in ice-cold Nonidet P-40 lysis buffer (10 mM HEPES (pH 7.4), 142.5 mM KCl, 0.2% Nonidet P-40, 5 mM EGTA), supplemented with 1 mM DTT, 12.5 mM β-glycerophosphate, 1 μM Na_3VO_4, 1 mM phenylmethylsulfonyl fluoride, and 1× protease inhibitor mix (Roche Molecular Biochemicals). Cell lysates were clarified by centrifugation and subjected to immunoprecipitation using specific antibodies and protein G or A beads. Immune complexes were resolved in SDS-polyacrylamide gels, transferred to polyvinylidene difluoride membranes (Millipore), and immunoblotted with antibodies, followed by detection with ECL (Amersham Pharmacia Biotech). Alternatively, lysates were analyzed directly by immunoblotting after normalization for total protein content.

Recombinant Protein Production and Protein Binding Assays—A GST fusion protein containing the CARD of procaspase-9 was expressed from pGEX-4T-1 in XL1-BLUE cells. Cells were lysed in 60 ml of phosphate-buffered saline, pH 7.4, 1 mM DTT, 1 mM EDTA, 1 mM phenylmethylsulfonyl fluoride, and 100 μg/ml lysozyme and sonicated, and supernatants were clarified by centrifugation. The resultant supernatants were mixed with 5 ml of glutathione-Sepharose for 1 h. Glutathione-Sepharose was pelleted and the liquid decanted from the resin. The resin was then washed twice with phosphate-buffered saline, 1 mM DTT, 1 mM EDTA, and batch elutions were performed with (50 mM Tris (pH 8.8), 1 mM DTT, 1 mM EDTA, 10 mM reduced glutathione. The final protein solution was dialyzed against 50 mM Tris (pH 7.5), 1 mM DTT, 1 mM EDTA to remove reduced glutathione. Attempts to produce GST- or His_6-CARD of TUCAN in bacteria failed to produce properly folded protein (not shown).

In vitro translated (IVT) proteins were synthesized using the TnT Quick Coupled Transcription/Translation System (Promega). A total of 5 μg of pcDNA3-TUCAN or pcDNA3-HA-Apaf1-(1–420) plasmid DNA was incubated with 100 μl of TnT Master Mix in the presence of 50 μCi of L-[^{35}S]methionine at 30 °C for 90 min, thus producing proteins of similar length and ensuring that Apaf1 was in a conformation component to bind the CARD of procaspase-9. IVT proteins were normalized based on ^{35}S incorporation, and then aliquots were prescreened in SDS-polyacrylamide gels, and the volumes were further adjusted to normalize for input of equal counts of full-length ^{35}S-labeled TUCAN or Apaf1-(1–420). Purified GST-CARD/procaspase-9 or GST-control proteins immobilized on 20 μl of glutathione-Sepharose beads were then incubated with various normalized amounts of IVT proteins (2–10 μl) in 0.1 ml of binding buffer (10 mM HEPES, 140 mM KCl, 2.5 mM $MgCl_2$, 1 mM EGTA, and 0.1% Nonidet P-40) at 4 °C for 2 h. The beads were washed three times with 1 ml of binding buffer, and bound proteins were boiled in SDS-loading buffer and subjected to SDS-PAGE, followed by analysis of the dried gels using either a PhosphorImager (Molecular Dynamics, Inc., Sunnyvale, CA) or by exposure to x-ray film and scanning densitometry (NIH Image). Background binding to GST was subtracted from specific binding, and the ratio of TUCAN/Apaf1 binding to GST-CARD/procaspase-9 was determined, correcting for differences in the methionine content of TUCAN and Apaf1-(1–420), which have 9 and 13 methionines, respectively.

Tissue and Tumor Specimens—Normal human tissues for immunohistochemistry analysis were obtained from biopsy and autopsy specimens, fixed in Bouin's solution (Sigma), and embedded in paraffin. Colon carcinoma specimens were obtained from the Department of Pathology, Yonsei University, College of Medicine (Seoul, Korea). Tissue samples included 102 primary tumors derived from patients who presented between 1986 and 1996 with stage II disease (Duke's B-stage), as defined by the American Joint Committee on Cancer and Union Internationale Contre le Cancer (AJCC/UICC) criteria. All patients were treated by surgical resection of the involved segment of colon. No postoperative adjuvant chemotherapy was performed initially in all cases. However, chemotherapy was administered for some patients after relapse. Clinical data represent a median follow-up of 60 months.

Tissue Microarray Construction—To construct colon cancer microarrays, 2–5 cylinders of 1-mm diameter tissue were taken from representative areas of archival paraffin blocks containing 8% formalin-fixed tumor and arrayed into a new recipient paraffin block with a custom-built precision instrument (Beecher Instruments, Silver Spring, MD). Serial sections (4 μm) were applied to 3-aminopropyltriethoxysilane-coated slides (Sigma), as described (15).

Immunohistochemistry—Dewaxed tissue sections were immunostained using a diaminobenzidine-based detection method as described in detail, employing the Envision-Plus horseradish peroxidase system

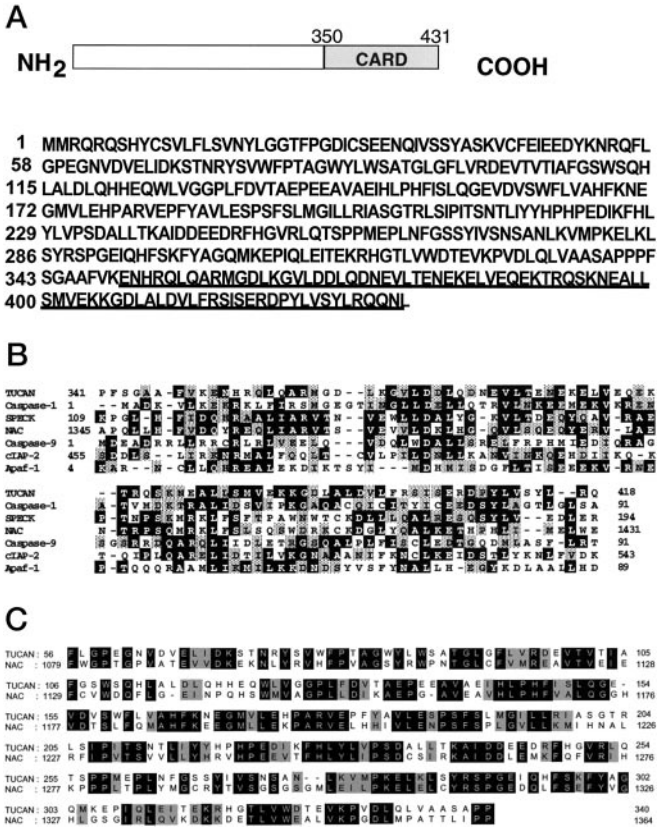

FIG. 1. **Structure and amino acid sequence of TUCAN.** *A*, the structure of TUCAN is depicted, showing the location of the CARD domain near the carboxyl terminus of the protein (*top*). The predicted amino acid sequence of the TUCAN protein is provided (bottom), with the CARD domain *underlined* using a *solid line* and the region displaying homology to NAC *underlined* with a *dashed line*. *B*, the sequence of the CARD of TUCAN was aligned with several other CARDs using ClustalW. Identical and similar residues are indicated in *black* and *gray*, respectively. *C*, a portion of the N-terminal region of TUCAN was aligned with a similar region in NAC.

(DAKO) using an automated immunostainer (Dako Universal Staining System) (14). Anti-TUCAN antibody was applied at 1:5000 (v/v). Incubation with antiserum preabsorbed with 5 μg/ml of either synthetic peptide (Bur215) or recombinant GST-CARD/TUCAN protein (Bur206) immunogen was used to verify specificity of the results. The scoring of tumor immunostaining was based on the percentage of immunopositive cells (0–100%) multiplied by staining intensity score (0, 1, 2, or 3), yielding scores of 0–300.

Statistical Analysis—Data were analyzed using the JMP Statistics software package (SAS Institute). An unpaired t test method and Pearson χ^2 test were used for correlation of TUCAN immunostaining data with the patient survival.

RESULTS

Identification of a New Member of the CARD Family—Using the CARD domain of Nod1 as a query, BLAST searches of the public data bases were performed, revealing an EST (KAI0955) containing an open reading frame for a 431-amino acid protein. The start codon initiating this open reading frame resides in a favorable context for translation (16) and was preceded by an in-frame stop codon. The predicted protein, which we have denominated as TUCAN (tumor-up-regulated CARD-containing antagonist of caspase-nine) for reasons explained below, contains a CARD located near its C terminus, preceded by a region lacking significant similarity to other recognizable domains (Fig. 1, *A* and *B*). The CARD of this protein is most similar to the CARD of Apaf1 (19% amino acid similarity), followed by CARD4 (Nod1) (18%), procaspase-9 (14%), and CED4 (12%) (Fig. 1*B*). The N-terminal region of this CARD family protein contains a segment (amino acids 50–350) sharing 50% amino acid sequence identity with a region in the proapoptotic protein NAC (DEPCAP) (Fig. 1*C*).

Searches of the recently released draft human genome data base (available on the Internet at www.ncbi.nlm.nih.gov) revealed that the gene encoding TUCAN resides on chromosome 19 and is predicted to contain 10 exons spread over 72 kilobase pairs. Reverse transcriptase-polymerase chain reaction analysis indicates that *TUCAN* mRNA is widely expressed in adult human tissues (available on the Internet at www.kazusa.or.jp/en/data base.html).

TUCAN Binds Selectively to Procaspase-9 and Itself—Since CARDs are known for their ability to bind each other, we tested TUCAN for interactions with the CARD-containing proteins procaspase-1, procaspase-2, procaspase-9, Apaf1, Nod1 (CARD4), CED4, NAC (DEFCAP), Cardiak (RIP2), Raidd (CRADD), Bcl10 (CIPER; huE10), cIAP1, cIAP2, CLAN, CARD9, and itself. Among these, TUCAN associated only with procaspase-9 and itself. Fig. 2 shows representative results from co-immunoprecipitation experiments that were performed using TUCAN containing either FLAG or Myc epitope tags expressed by transient transfection in HEK293T cells with epitope-tagged procaspase-9 or other proteins. An inactive mutant of procaspase-9 in which the catalytic cysteine was substituted with alanine ($Cys^{287} \rightarrow Ala$) was employed for these experiments to avoid induction of apoptosis (17). Cell lysates were then prepared, and immunoprecipitations were performed using anti-FLAG or anti-Myc antibodies, followed by SDS-PAGE/immunoblot analysis. TUCAN co-immunoprecipitated with procaspase-9 but not the CARD-containing protein Apaf1 (Fig. 2). TUCAN also did not co-immunoprecipitate with the CARD-containing proteins procaspase-1, procaspase-2, Nod1, CED4, NAC, Cardiak, Raidd, Bcl10, CLAN, CARD9, cIAP1, and cIAP2 (not shown). Moreover, TUCAN did not associate nonspecifically with caspases, since co-immunoprecipitation experiments failed to demonstrate interactions with the DED-containing caspases, procaspase-8 and -10 (Fig. 2*A*).

To explore the role of the CARD domain within TUCAN for interactions with procaspase-9, fragments of TUCAN were expressed consisting of essentially only the CARD (residues 345–431) or lacking the CARD (residues 1–337). Procaspase-9 co-immunoprecipitated with full-length TUCAN and the CARD-only fragment but not the ΔCARD fragment of TUCAN (Fig. 2*B*). Thus, the CARD domain of TUCAN is necessary and sufficient for association with procaspase-9.

Self-association of TUCAN was also confirmed by co-immunoprecipitation experiments, using HA- and Myc-tagged proteins and contrasting the full-length, CARD-only, and ΔCARD proteins. Full-length TUCAN interacted with full-length TUCAN and the CARD-only fragment but not the ΔCARD fragment (Fig. 2*C* and data not shown). Thus, the CARD domain of TUCAN is necessary and sufficient for self-association.

Comparison of the CARDs of TUCAN and Apaf1—Similar to Apaf1, TUCAN binds selectively to procaspase-9, as shown above. We therefore compared the surface topology of the CARD of Apaf1 with a three-dimensional model of the CARD of TUCAN (Fig. 3*A*). The reported structure of the CARD of Apaf1 in complex with the CARD of procaspase-9 has revealed that Asp^{27}, Ser^{31}, Glu^{40}, and Glu^{41} in Apaf1 make important contacts with the CARD of procaspase-9, forming mainly a hydrogen bond network constituted of 9 hydrogen bonds (18). Three of these four critical residues are identical or involve conservative replacements in the CARD of TUCAN, corresponding to Asp^{367}, Asp^{371}, and Glu^{381} (Fig. 3*A*). Among these, Asp^{27} in the CARD of Apaf1 makes the most contributions to interactions with procaspase-9 (five hydrogen bonds), while Ser^{31} and Glu^{40} contribute two hydrogen bonds each (18). In TUCAN, Lys^{380}

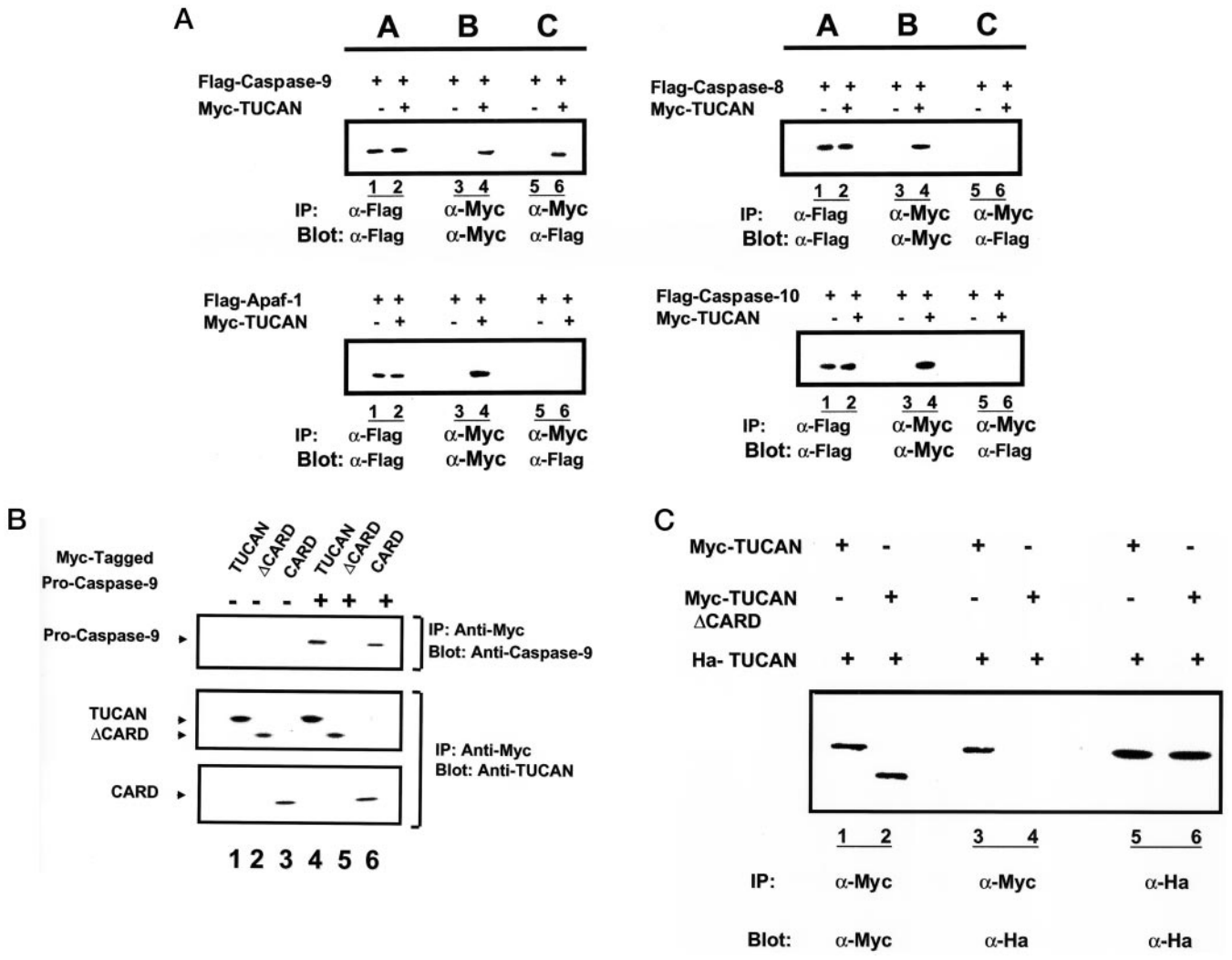

FIG. 2. **TUCAN associates with itself and procaspase-9.** Co-immunoprecipitation assays were performed essentially as described (17), using lysates prepared from HEK293T cells that had been transiently transfected 1 day prior with plasmids encoding various epitope-tagged proteins as indicated. Immunoprecipitates (*IP*) were analyzed by SDS-PAGE/immunoblotting, using an ECL method for antibody detection. *A*, HEK293T cells were transfected with plasmids encoding Myc-tagged TUCAN or FLAG-procaspase-9 ($Cys^{287} \rightarrow Ala$), FLAG-Apaf1, FLAG-procaspase-8 ($Cys^{360} \rightarrow Ala$), or FLAG-procaspase-10 (Cys^{358} Ala). *B*, HEK293T cells were transfected with plasmids encoding procaspase-9 ($Cys^{287} \rightarrow Ala$) and either Myc-tagged TUCAN, CARD only (residues 345–431), or ΔCARD (residues 1–337). Anti-Myc immunoprecipitates were analyzed by blotting using rabbit antisera specific for caspase-9 (14) or antisera raised against a synthetic peptide corresponding to residues 126–147 of the TUCAN protein (Bur215) (*top*) or against a GST fusion protein representing the CARD domain of TUCAN (residues 345–431) and Bur206 (*bottom*). *C*, HEK293T cells were transfected with plasmids encoding HA-tagged TUCAN together with either Myc-tagged full-length TUCAN or a truncation mutant lacking the CARD domain (ΔCARD).

substitutes for Glu^{40} in the model, which would eliminate one or possibly two hydrogen bonds and thus weaken interactions with the CARD of procaspase-9. However, inspection of the reported CARD-CARD (Apaf1/procaspase-9) structure suggests that Lys^{380} at this position would not be detrimental to the other known interactions involving Asp^{27}, Ser^{31}, and Glu^{41}, thus preserving seven of the nine hydrogen bonds (not shown). Also, while the hydrogen bonding would be different for TUCAN/procaspase-9 CARD-CARD complexes compared with Apaf-1/procaspase-9 complex because of Lys^{380}, the possibility of making other hydrogen bonds between this lysine and other amino acids in the CARD of procaspase-9 cannot be excluded. Thus, these comparative modeling studies suggest that most of the amino acids of Apaf1 involved in CARD-CARD interactions with procaspase-9 are conserved in TUCAN, supporting the experimental data demonstrating specific association of TUCAN with procaspase-9.

To contrast the relative affinity of TUCAN and Apaf1 for binding to the CARD of procaspase-9, we performed *in vitro* protein binding assays. For binding experiments, therefore, affinity-purified GST-control protein or GST-CARD/caspase-9 was incubated with various amounts of ^{35}S-labeled TUCAN or Apaf1 (residues 1–420), which had been prepared by *in vitro* translation and normalized. Both Apaf1-(1–420) and TUCAN exhibited concentration-dependent and specific binding to GST-CARD/caspase-9, although Apaf1-(1–420) also displayed some nonspecific binding to GST control (Fig. 3*B*). From these comparisons, TUCAN was estimated to bind the CARD of procaspase-9 with an affinity of 0.45–0.62× relative to Apaf1, based on quantification of the amounts of bound ^{35}S-labeled proteins by PhosphorImager analysis ($n = 2$), after correction for background binding to GST-control and for differences in the methionine content of the TUCAN and Apaf1-(1–420) proteins. Thus, TUCAN appears to bind the CARD of procaspase-9 with an affinity comparable with Apaf1.

TUCAN Competes with Apaf1 for Binding to Procaspase-9—The ability of TUCAN to associate with procaspase-9 raised the question of whether this protein might compete for binding with Apaf1 in cells. To explore this possibility, HEK293T cells were transiently transfected with increasing amounts of plas-

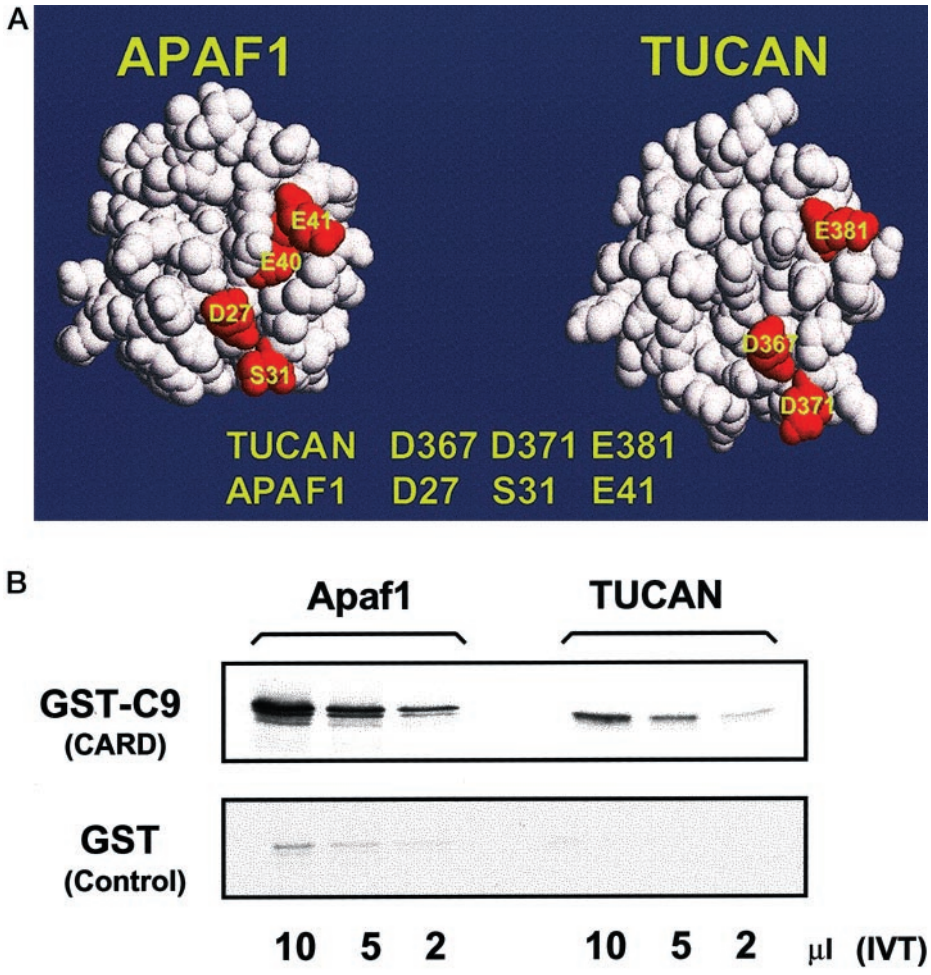

FIG. 3. **Comparison of the CARDs of TUCAN and Apaf1.** *A*, a three-dimensional model of the CARD of TUCAN was generated using FFAS and MODELLER, and compared with the reported structure of the CARD of Apaf1 (18). The residues on the surface of the Apaf1 CARD, which make important contacts with the CARD of procaspase-9 are indicated in *red* (18) and compared with the corresponding residues in the CARD of TUCAN. *B*, GST-CARD/procaspase-9 (*top*) or GST (*bottom*) protein (1 μg) immobilized on 20 μl of glutathione-Sepharose was incubated with 2, 5, or 10 μl of IVT ^{35}S-labeled TUCAN or Apaf1-(1–420), normalized by PhosphorImaging prior to use. Bound IVT proteins were analyzed by SDS-PAGE/autoradiography.

mid DNA encoding TUCAN and fixed amounts of plasmids encoding FLAG-tagged procaspase-9 ($Cys^{287} \rightarrow Ala$) and Myc-tagged Apaf1 (residues 1–560), an Apaf1 mutant that is constitutively active in the absence of cytochrome *c* (19). Co-immunoprecipitation experiments were then performed using lysates from these transfected cells, in which Apaf1/procaspase-9 interactions were monitored by immunoprecipitating Myc-Apaf1 and detecting associated procaspase-9 by SDS-PAGE/immunoblot assay. In the absence of TUCAN, association of procaspase-9 with Myc-Apaf1 was readily detected. In contrast, expressing TUCAN in HEK293T cells resulted in dose-dependent reductions in the relative amounts of procaspase-9 that co-immunoprecipitated with Myc-Apaf1 (Fig. 4). The total amounts of procaspase-9 ($Cys^{287} \rightarrow Ala$) and Myc-Apaf1-(1–560) present in lysates were not altered by TUCAN (Fig. 4), thus confirming a specific defect in Apaf-1/procaspase-9 association caused by overexpressing the TUCAN protein.

TUCAN Inhibits Caspase Activation by Cytochrome c—Apaf1 functions as a cytochrome *c*-dependent activator of caspase-9 (20). Since TUCAN interferes with binding of Apaf1 to procaspase-9, we explored whether overexpression of this protein inhibits activation of caspases by cytochrome *c* in cell extracts. Accordingly, HEK293T cells were transiently transfected with either control or Myc-TUCAN-producing plasmids, and cytosolic extracts were prepared, normalized for total protein content, and then treated with 10 μM cytochrome *c* and 1 mM ATP to induce activation of Apaf1 (12, 20). In control extracts, cytochrome *c* induced activation of caspases, as measured by cleavage of the fluorogenic caspase substrate Ac-DEVD-AFC (Fig. 5*A*). By comparison, far less caspase activity was induced by cytochrome *c* in extracts prepared from TUCAN-transfected

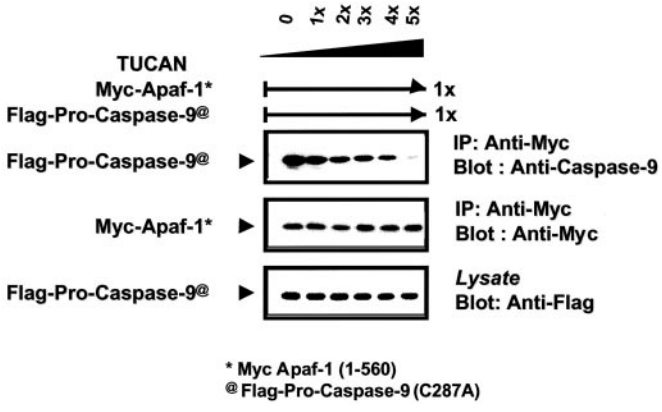

FIG. 4. **TUCAN interferes with Apaf1 association with procaspase-9.** HEK293T cells (100-mm dish) were transfected with 2 μg of pcDNA3-FLAG-procaspase-9 ($Cys^{287} \rightarrow Ala$); 2 μg of pcDNA3-Myc-Apaf1-(1–560); and 0, 2, 4, 6, or 8 μg of pcDNA3-HA-TUCAN, normalizing total DNA to 12 μg using empty pcDNA3. After 2 days, cell lysates were prepared, and immunoprecipitation was performed using anti-Myc monoclonal antibody, followed by SDS-PAGE/immunoblot analysis using anticaspase-9 antiserum (*top*) or anti-Myc antibody (*middle*). Lysates were also run directly in a gel and analyzed by immunoblotting using anti-FLAG monoclonal antibody.

cells. Immunoblot analysis of an aliquot of the extracts using anti-TUCAN antiserum confirmed production of the protein in cells transfected with pcDNA3-Myc-TUCAN but not control plasmid (Fig. 5*A*). In contrast to cytochrome *c*, caspase activity induced by the addition of granzyme B (GraB) was equivalent in extracts prepared from control- and TUCAN-expressing cells

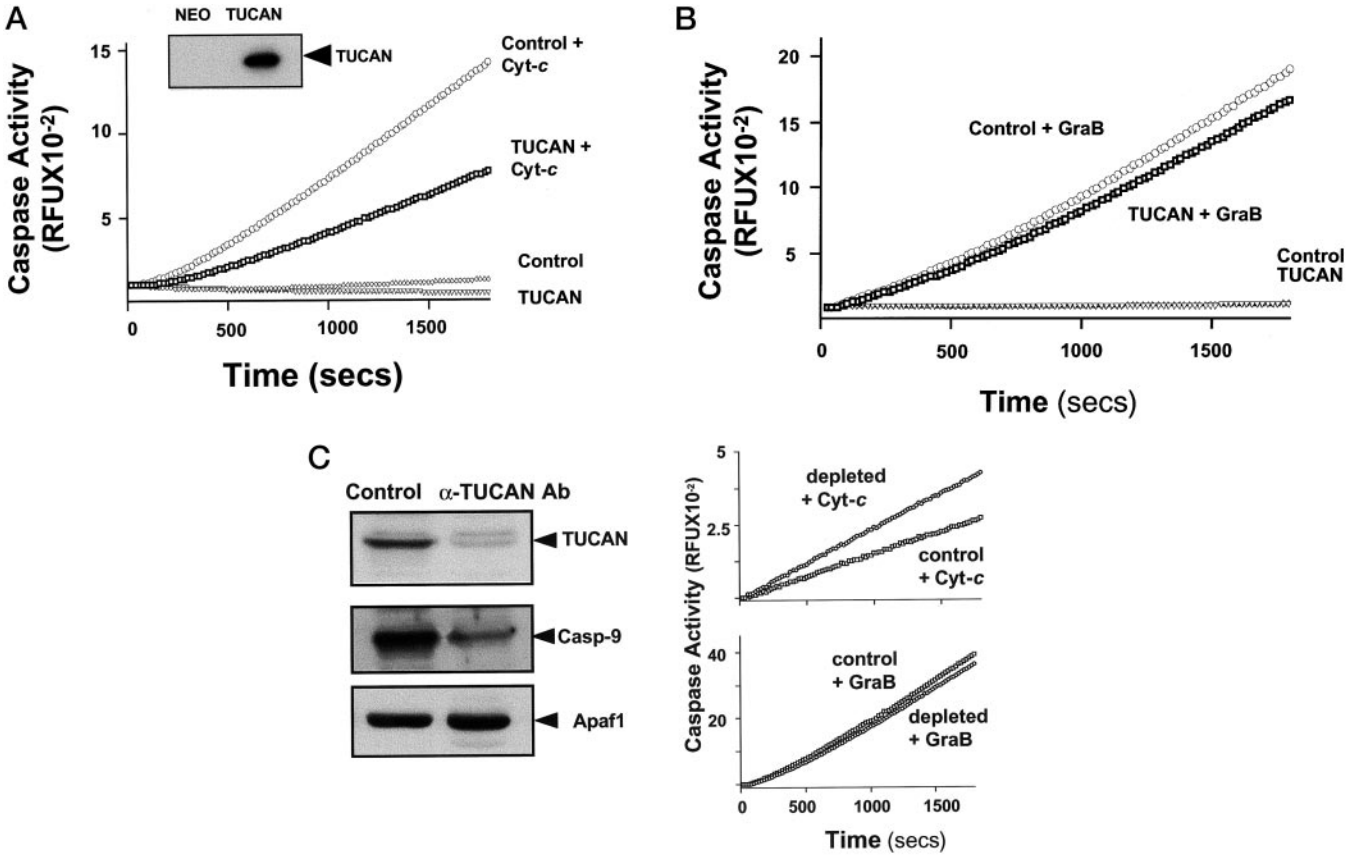

FIG. 5. **TUCAN inhibits caspase activation induced by cytochrome *c*.** *A*, HEK293T cells (100-mm dish) were transiently transfected with 3 μg of pcDNA3 or pcDNA3-TUCAN. Lysates were prepared as described (12), normalized for total protein content, and either analyzed by SDS-PAGE/immunoblotting using anti-TUCAN antiserum (Bur206) or used for caspase activation assays. For caspase activity measurements, either 10 μM cytochrome *c* and 1 mM dATP (*A*) or 10 ng of GraB (*B*) were added, and extracts were incubated at 30 °C for 0.5 h. Then 100 μM Ac-DEVD-AFC substrate was added, and generation of fluorogenic AFC was measured (relative fluorescence units (*RFU*)) continuously by spectrofluorimetry, as described (12). *C* and *D*, MCF7 cell extracts were immunodepleted using anti-TUCAN antisera (combination of Bur206 and Bur215) or preimmune serum (control), and then equivalent volumes were either analyzed by SDS-PAGE/immunoblotting using antisera specific for TUCAN (Bur206), procaspase-9, or Apaf1, with ECL-based detection (*C*), or employed for caspase activity assays, where lysates were supplemented with procaspase-3, prior to the addition of either 10 μM cytochrome *c* and 1 mM dATP (*top*) or 10 ng granzyme B (*bottom*) (*D*). Generation of fluorescent AFC from Ac-DEVD-AFC substrate was monitored continuously by spectrofluorimetry.

(Fig. 5*B*). Since GraB directly cleaves and activates many caspase family zymogens (21), this observation demonstrates that TUCAN-overexpressing cells do not have an overall defect in caspase activation mechanisms, thus confirming the specificity of these results.

Although overexpression of TUCAN suppressed caspase activation induced by cytochrome *c*, we complemented these experiments by exploring the role of the endogenous TUCAN protein through immunodepletion experiments. Accordingly, cytosolic extracts from MCF-7 cells (which contain high endogenous levels of TUCAN protein (see below)) were incubated with anti-TUCAN antiserum or control preimmune rabbit serum, and then immune complexes were removed by adsorption to protein A-Sepharose. Immunoblot analysis confirmed marked reductions in the levels of endogenous TUCAN protein from lysates (Fig. 5*C*). Levels of procaspase-9 were also decreased, consistent with the observation that TUCAN forms complexes with this protein. In contrast, Apaf1 levels were unaffected by the immunodepletion procedure. Functional comparison of cytosolic extracts that had been depleted with anti-TUCAN *versus* preimmune sera with respect to cytochrome *c*-mediated activation of caspases demonstrated that removal of TUCAN was associated with a gain in cytochrome *c* inducibility of extracts (Fig. 5*D*). Thus, despite co-depletion of some of the procaspase-9 from extracts, immunodepletion of TUCAN resulted in a net increase in the ability of cytochrome *c* to activate caspase, thus supporting a role for TUCAN as an endogenous suppressor of cytochrome *c*-mediated procaspase-9 activation.

TUCAN Inhibits Induction of Apoptosis by Caspase-9-dependent Stimuli in Transient Transfection Assays—Apoptosis can be induced by co-expressing procaspase-9 and Apaf1 in HEK293T cells (22), thus providing an opportunity to assess whether TUCAN can block caspase-9-dependent apoptosis. Accordingly, HEK293T cells were transfected with plasmids encoding procaspase-9, Apaf1, or TUCAN, alone and in various combinations, and then apoptosis was measured 24 h later based on DAPI staining of fixed cells. In the absence of TUCAN, the combination of procaspase-9 and Apaf1 induced apoptosis of nearly half the transfected cells (Fig. 6*A*). In contrast, co-transfecting cells with a TUCAN-producing plasmid reduced apoptosis to background levels. Moreover, the CARD domain of TUCAN was sufficient for suppression of apoptosis induced by the combination of procaspase-9 and Apaf1 (Fig. 6*A*).

The proapoptotic protein Bax induces release of endogenous cytochrome *c* from mitochondria, triggering apoptosis through an Apaf1- and caspase-9-dependent mechanism (reviewed in Ref. 23). We therefore tested the effects of TUCAN overexpression on apoptosis induced by transient transfection of HEK293T cells with a Bax-producing plasmid. As shown in Fig. 6*B*, expressing Bax in HEK293T cells induced apoptosis of over

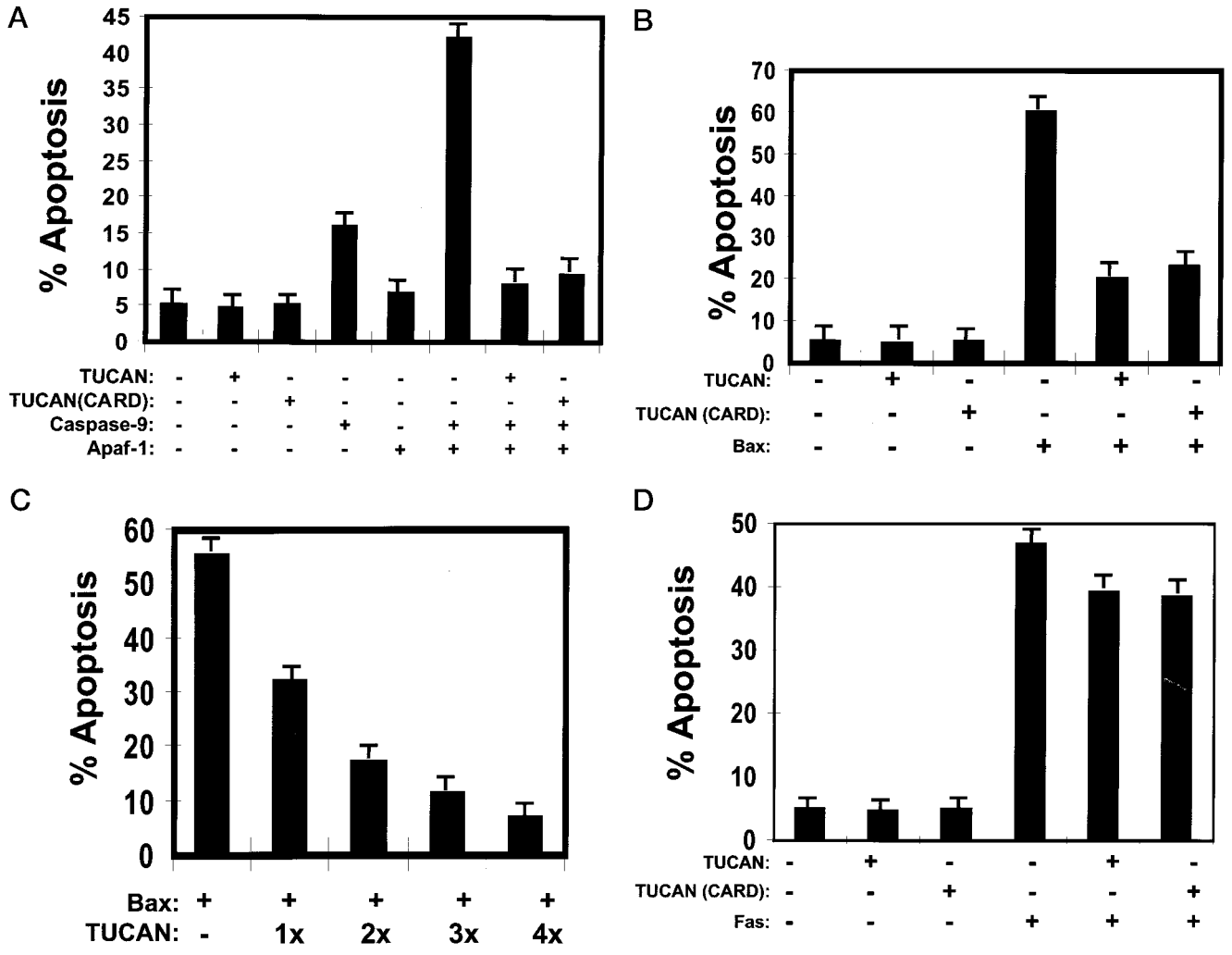

FIG. 6. **TUCAN suppresses apoptosis induction by caspase-9-dependent stimuli in transient transfection assays.** *A*, HEK293 cells (60-mm dish) were transfected with 1 μg each of pcDNA3-Myc-TUCAN, pcDNA3-Myc-CARD/TUCAN, pcDNA3-FLAG-procaspase-9, pcDNA3-HA-Apaf1, or combinations of the same, normalizing total DNA to 3.5 μg using empty pcDNA3. After 24 h, cells were fixed and stained with DAPI, and the percentage of apoptotic cells was determined by UV microscopy (mean ± S.D.; $n = 3$). *B*, HEK293 cells (60-mm dish) were transfected with 1 μg each of pcDNA3-Myc-TUCAN or pcDNA3-Myc-CARD/TUCAN, either alone or in the presence of 1 μg of pcDNA3 Bax, normalizing total DNA to 3.5 μg using empty pcDNA3. After 24 h, cells were fixed and stained with DAPI, and the percentage of apoptotic cells was determined by UV microscopy. *C*, HEK293 cells (60-mm dish) were transfected with 1 μg of pcDNA3-Bax in the presence or absence of 1, 2, 3, or 4 μg of pcDNA3-Myc-TUCAN, normalizing the DNA to 5 μg with pcDNA3. After 24 h, cells were fixed and stained with DAPI, and the percentage of apoptotic cells was determined (mean ± S.D.; $n = 3$). *D*, HEK293 cells (60-mm dish) were transfected with 1 μg each of pcDNA3-Myc-TUCAN, pcDNA3-Myc TUCAN/CARD, either alone or in the presence of 1 μg of pcDNA3-Fas, normalizing total DNA to 3.5 μg using empty pcDNA3. After 24 h, cells were fixed and stained with DAPI, and the percentage of apoptotic cells was determined by UV microscopy (mean ± S.D.; $n = 3$).

half of the transfected cells. In contrast, co-expressing TUCAN with Bax markedly reduced the percentage of cells undergoing apoptosis. Immunoblot analysis confirmed that TUCAN did not interfere with expression of the Bax protein (not shown). The CARD domain of TUCAN was sufficient for suppressing Bax-induced apoptosis (Fig. 6*B*). Moreover, experiments in which TUCAN-producing plasmid DNA was transfected in ratios ranging from 1:1 to 4:1 relative to Bax-encoding plasmid DNA demonstrated dose-dependent inhibition of Bax-induced apoptosis (Fig. 6*C*).

In contrast to Bax, the death receptor Fas (CD95) triggers apoptosis by an Apaf1- and caspase-9-independent mechanism (24, 25). Apoptosis induced by transient overexpression of Fas in HEK293T cells was not suppressed by TUCAN (Fig. 6*D*), thus demonstrating that TUCAN selectively blocked certain apoptotic pathways.

Stable Overexpression of TUCAN Renders Cells More Resistant to Apoptosis Induced by Caspase-9-dependent Stimuli—To further explore the role of TUCAN as an apoptosis suppressor, Jurkat T cells were stably transfected with either control or TUCAN-encoding plasmids. Immunoblot analysis of the resulting cell lines using anti-TUCAN antiserum demonstrated overexpression of Myc-TUCAN protein in Jurkat cells harboring the pcDNA3-Myc-TUCAN plasmid but not the pcDNA3-Myc control plasmid (Fig. 7*A*).

Since the anti-cancer drug VP16 (etoposide) and the kinase inhibitor staurosporine (STS) have been shown to induce apoptosis through an Apaf1- and caspase-9-dependent mechanism (24–26), these stimuli were compared in the control- and TUCAN-overexpressing Jurkat transfectants. As shown in Fig. 7*A*, significantly less cell death was induced by VP16 and STS in TUCAN-overexpressing compared with control-transfected Jurkat cells. In contrast to VP16 and STS, cell death induced by anti-Fas antibody was not suppressed by overexpression of TUCAN, consistent with data demonstrating that Fas can trigger apoptosis independently of Apaf1 and caspase-9 (24, 25). These differences in cell death induction were associated with comparable changes in caspase activity, measured in lysates

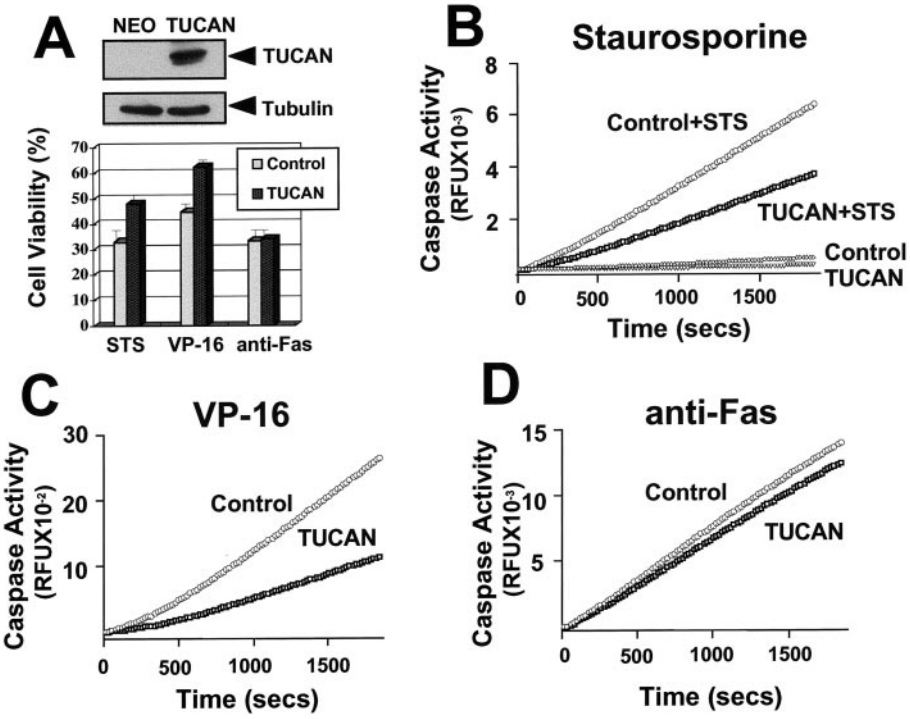

FIG. 7. **Stable overexpression of TUCAN renders cells more resistant to cell death and caspase activation induced by caspase-9-dependent stimuli.** Jurkat T cells were stably transfected with pcDNA3 or pcDNA3-Myc-TUCAN plasmid DNA. *A* (*top*), immunoblot analysis was performed using 10 μg of total protein from Jurkat-Neo (control) and Jurkat-TUCAN cells. The blot was probed with anti-TUCAN (Bur206–11) antibody to detect TUCAN or with anti-tubulin antibody to verify loading of equivalent amounts of total protein. *A* (*bottom*), The stable transfectants of Jurkat harboring pcDNA3 (control) and pcDNA3-Myc-TUCAN plasmids were treated for 16 h with 0.1 μM STS, 10 μM VP-16, or 0.1 μg/ml CH11 antibody (anti-Fas). Cell viability was determined by trypan blue dye exclusion assay (mean ± S.D.; $n = 3$). Production of TUCAN protein was analyzed by SDS-PAGE followed by immunoblotting using anti-TUCAN (Bur206) or anti-tubulin antibodies. *B–D*, caspase activity was measured in lysates prepared from Jurkat-Neo (control) and Jurkat-TUCAN stable transfectants after a 3-h culture in the presence or absence of 0.1 μM staurosporine (*B*), 10 μM VP16 (*C*), or 0.1 μg/ml CH11 antibody (anti-Fas) (*D*). Release of fluorogenic AFC from the caspase substrate Ac-DEVD-AFC was measured continuously, expressing data as relative fluorescence units (*RFU*)/μg of total protein.

prepared from Jurkat transfectants after treatment with VP16, STS, or anti-Fas antibody. Specifically, when VP16 or STS was used as the stimulus, DEVD-cleaving caspase activity was reduced in TUCAN-overexpressing Jurkat cells compared with control-transfected cells (Fig. 7, *B* and *C*). In contrast, when anti-Fas was the stimulus, comparable amounts of caspase activity were measured in TUCAN-overexpressing and control-transfected Jurkat cells (Fig. 7*D*). Moreover, the addition of GraB to extracts from stable Jurkat transfectants (which had not received a prior apoptotic stimuli) also resulted in essentially equivalent amounts of caspase activity (not shown), further demonstrating the selectivity of TUCAN and confirming that alternative pathways for caspase activation remain intact.

Endogenous TUCAN Is Expressed in Cancer Cell Lines—Some antiapoptotic proteins are produced at high levels in cancers, conferring apoptosis resistance (reviewed in Ref. 27). To gain preliminary insights into the expression of TUCAN in cancers, the NCI (National Institutes of Health) panel of 60 human tumor cell lines (28) was analyzed by immunoblotting using an antiserum specific for TUCAN (Fig. 8*A*). Lysates were normalized for total protein content prior to analysis. Relative levels of TUCAN protein varied widely among the tumor lines tested, with some cell lines containing especially abundant levels of this protein such as MCF7 breast cancer, OVCAR5 ovarian cancer, and NCI-H322M lung cancer cells. In some of these tumor lines, TUCAN migrated in SDS-PAGE as a broad band or as an apparent doublet, suggesting the possibility of post-translational modifications that remain to be characterized (Fig. 8*A*).

Next, the levels of endogenous TUCAN protein in some of these cancer cell lines were compared with the transfected

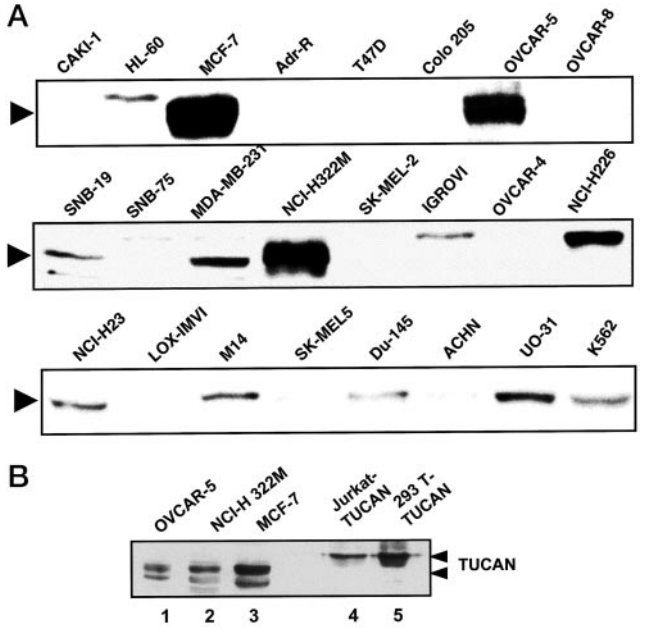

FIG. 8. **Expression of endogenous TUCAN in tumor cell lines.** *A*, examples of immunoblot data are shown for several human tumor cell lines within the NCI 60-tumor cell line panel. In all cases, lysates were normalized for total protein content (50 μg) prior to SDS-PAGE/immunoblot assay using anti-TUCAN antiserum Bur206. *B*, levels of endogenous and exogenous TUCAN were compared by immunoblotting (10 μg of total protein) for the tumor lines OVCAR5, NCI-H322M, and MCF7, *versus* stably transfected Jurkat-TUCAN and transiently transfected HEK293T-TUCAN cells. The position of the TUCAN band migrates slower in SDS-PAGE for the transfected cells due to the presence of a Myc epitope tag.

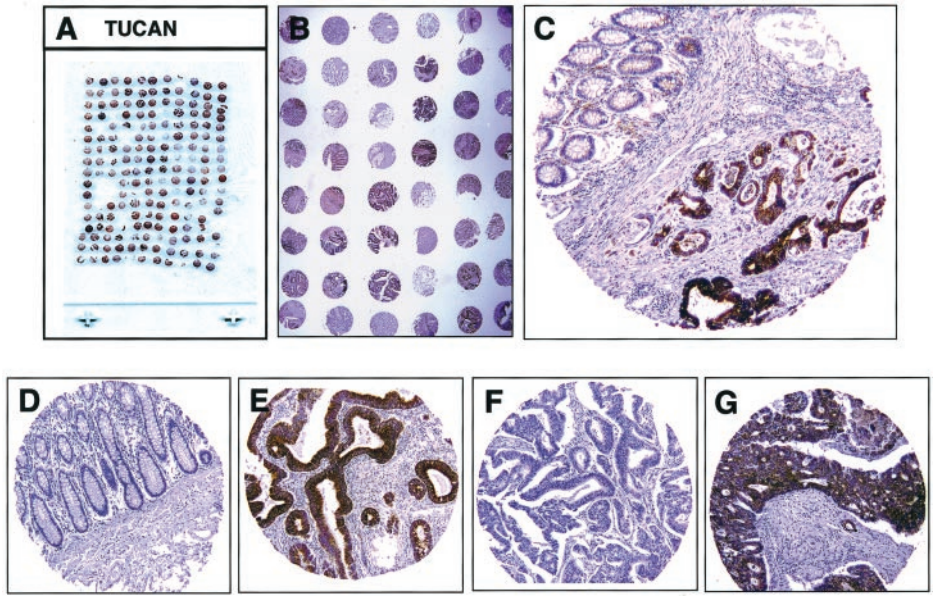

FIG. 9. **Immunohistochemical analysis of TUCAN expression in colorectal cancer.** Representative TUCAN immunostaining results are presented for a tissue microarray of colorectal carcinoma specimens. A tissue microarray block was prepared using 1-mm diameter cylindrical punches of fixed tissue from 102 colon tumor specimens. The microarray was immunostained using rabbit antisera raised against either synthetic TUCAN peptide (Bur215) or recombinant TUCAN protein (Bur206). Colorimetric detection of antibody was accomplished using a diaminobenzidine-based method (*brown*). Nuclei were counterstained with hematoxylin (*blue*). Both anti-TUCAN antibodies (Bur206 (*A–C*) and Bur215 (*D–G*)) were used for immunostaining analysis in duplicate, yielding similar results. *A* and *B*, TUCAN immunostaining in the array of colorectal cancer specimens is presented at × 5 and × 20 magnification. *C*, an example is shown of a tumor specimen in which invasive cancer with strong intensity TUCAN immunostaining (*bottom*, *right*) is juxtaposed with normal colonic epithelium (*upper*, *left*), which contains low intensity TUCAN staining (250×). *D–G*, examples are provided of TUCAN immunostaining results in normal mucosa (*D*) and three different colon carcinomas (*E–G*), representing the diversity of TUCAN immunostaining intensities seen in these patient materials (*150*×).

TABLE I
Summary of TUCAN immunostaining results for colon cancer

Archival tumor specimens were immunostained for TUCAN. Data shown here were obtained using Bur206 antiserum, but similar results were also obtained using Bur215, thus confirming the results (not shown). Statistical significance was determined by analysis of variance/*t* test comparing the group of dead patients ($n = 31$) with those still surviving ($n = 71$).

Patient status	*n*	Immunopositivity		Immunointensity		Immunoscore	
		Mean ± S.E.	Median	Mean ± S.E.	Median	Mean ± S.E.	Median
		%	%				
Alive without disease	61	58 ± 3	60	1.4 ± 0.1	1	92 ± 9	80
Alive with disease	10	54 ± 7	55	1.3 ± 0.2	1	73 ± 21	65
Dead from disease	31	90 ± 4	95	2.5 ± 0.1	3	224 ± 12	240
p values	102	$p < 0.0001$		$p < 0.0001$		$p < 0.0001$	

HEK293T and Jurkat cells. The levels of plasmid-derived TUCAN produced in transiently transfected HEK293T cells were comparable with the endogenous levels of TUCAN found in MCF7 breast cancer cells (Fig. 8*B*). Levels of plasmid-derived TUCAN produced in the stably transfected Jurkat cells were comparable in amount with endogenous TUCAN measured in OVCAR5 ovarian and NCI-H322M lung cancer cell lines. We conclude from these observations that the levels of TUCAN produced by transfection are similar to those that occur endogenously in some tumor cell lines.

TUCAN Expression Is Elevated in Colon Cancers and Correlates with Shorter Patient Survival—Using anti-TUCAN antibodies, the expression of this antiapoptotic protein was analyzed by immunohistochemical methods in a collection of 102 archival paraffin-embedded colon cancer specimens derived from patients with uniform clinical stage (Duke's B; stage II) and treatment (surgery without adjuvant chemotherapy). A tissue microarray was constructed so that all 102 tumor specimens could be analyzed on a single glass slide, thus minimizing differences in immunointensity due to technical artifacts (Fig. 9).

Of these 102 tumor specimens arrayed, 66 contained adjacent normal colonic epithelium in the same section, permitting comparisons of the intensity of TUCAN immunostaining in tumor *versus* normal cells. TUCAN immunointensity was stronger in the invasive cancer cells compared with normal colonic epithelial cells in 42 of 66 (64%) of these specimens, suggesting that roughly two-thirds of colon cancers up-regulate their levels of TUCAN protein. TUCAN immunoreactivity was present diffusely through the cytosol of these cells (Fig. 9). Control stainings performed with either preimmune serum or with anti-TUCAN antiserum that had been preabsorbed with TUCAN immunogen confirmed the specificity of these results (not shown).

Tumor immunostaining results were scored with respect to immunointensity (ranked on a scale of 0–3), percentage immunopositivity (0–100%), and immunoscore (which is the product of immunointensity and immunopercentage), and these data were correlated with patient survival information. TUCAN immunostaining was significantly higher among patients who died of their cancer ($n = 31$), compared with patients who remained alive without disease ($n = 61$) or alive with recurrent disease ($n = 10$) (Table I). No correlation of TUCAN immunostaining with tumor histology was found (not shown). We conclude therefore that TUCAN expression is abnormally elevated in a substantial proportion of early

stage colon cancers, apparently correlating with shorter patient survival.

DISCUSSION

We have identified a new member of the human CARD family, which we have termed TUCAN (for tumor-up-regulated CARD-containing antagonist of caspase-nine. The TUCAN protein binds specifically to procaspase-9 and interferes with its interaction with Apaf1, thereby squelching apoptosis signaling in the mitochondrial/cytochrome *c* pathway. TUCAN overexpression reduces apoptosis induced by stimuli that are known to activate the mitochondrial pathway for caspase activation, including Bax, DNA-damaging drugs, and staurosporine. In contrast, apoptosis induced via alternative pathways, including GraB and Fas (tumor necrosis factor family death receptor), is not inhibited by TUCAN.

The sequence of TUCAN was first publicly disclosed as EST clone KIAA0955 (available on the Internet at www.kazusa.or.jp/en/data base.html), resulting from random sequencing of brain cDNAs (29). Several other groups have recently deposited the same predicted protein sequence into GenBank™ under various names, including CARD8 (GenBank™ accession number AF322184.1, gi:12247742), NDPP1 (AF331519.1, gi:12658408), and DACAR (AY026322.1, gi:13027707), in addition to KIAA0955. This report, however, represents the first functional characterization of this protein, including the first demonstration that this protein is actually produced in cells, and its predicted CARD displays CARD-like behavior, namely binding to the CARDs of other proteins (*e.g.* procaspase-9).

The CARD domain of TUCAN is sufficient for binding procaspase-9 and suppressing caspase-9-dependent apoptosis. However, TUCAN also contains an N-terminal domain that lacks similarity to other recognizable domains. This region of the TUCAN protein shares amino acid similarity with a segment of the NAC protein, a CARD-carrying regulator of the Apaf1 apoptosome (30, 31). The function of this domain is presently unknown, but it theoretically could serve to regulate TUCAN in a variety of ways, such as controlling interactions with other proteins, affecting protein degradation, or altering protein subcellular location. Interestingly, the N-terminal (non-CARD) region of TUCAN contains several candidate phosphorylation sites, including PKC (S/T-*X*-R/K) sites at amino acids 72, 286, 313, and 416, Casein kinase II (S/T-*X*-D/E) sites at 289, 376, 398, 414, and 416 and mitogen-activated protein kinase/cyclin-dependent kinase (S/T-P) sites at 187 and 289. When taken together with evidence of multiple forms of TUCAN based on mobility in SDS-PAGE experiments, we speculate that post-translational modifications of this protein may play a role in regulating TUCAN function. Interestingly, TUCAN also contains a candidate caspase cleavage site (DEED) at residues 243–246.

Relatively high levels of TUCAN are found in several human cancer cell lines. Moreover, compared with normal colonic mucosa, TUCAN immunostaining was pathologically elevated in roughly two-thirds of early stage colon cancers, providing evidence of abnormal overexpression of this antiapoptotic protein in association with malignant transformation. Previous data from use of cells derived from Apaf1 and procaspase-9 knockout mice have provided evidence that these proapoptotic proteins function as tumor suppressors in a p53-dependent pathway (32). Overexpression of TUCAN should be functionally equivalent to loss of Apaf1 or procaspase-9, suggesting that elevated levels of TUCAN could promote tumor pathogenesis or progression. Consistent with this notion, colon cancer patients whose tumors contained higher levels of TUCAN were more likely to die from their disease, based on retrospective analysis using archival specimens. Further analysis of the expression and function of TUCAN in tumors therefore is warranted.

Acknowledgment—We thank R. Cornell for manuscript preparation.

REFERENCES

1. Vaux, D., and Korsmeyer, S. (1999) *Cell* **96,** 245–254
2. Thompson, C. B. (1995) *Science* **267,** 1456–1462
3. Salvesen, G. S., and Dixit, V. M. (1997) *Cell* **91,** 443–446
4. Thornberry, N., and Lazebnik, Y. (1998) *Science* **281,** 1312–1316
5. Salvesen, G. S., and Dixit, V. M. (1999) *Proc. Natl. Acad. Sci. U. S. A.* **96,** 10964–10967
6. Hofmann, K., Bucher, P., and Tschopp, J. (1997) *Trends Biochem. Sci.* **22,** 155–156
7. Zou, H., Henzel, W. J., Liu, X., Lutschg, A., and Wang, X. (1997) *Cell* **90,** 405–413
8. Altschul, S. F., Madden, T. L., Schaeffer, A. A., Zhang, J., Zhang, Z., Miller, W., and Lipman, D. J. (1997) *Nucleic Acids Res.* **25,** 3389–3402
9. Li, W., Pio, F., Pawlowski, K., and Godzik, A. (2001) *Bioinformatics*, in press
10. Rychlewski, L., Jaroszewski, L., Li, W., and Godzik, A. (2000) *Protein Sci.* **9,** 232–241
11. Sali, A., and Blundell, T. L. (1993) *J. Mol. Biol.* **234,** 779–815
12. Deveraux, Q. L., Takahashi, R., Salvesen, G. S., and Reed, J. C. (1997) *Nature* **388,** 300–304
13. Krajewska, M., Wang, H.-G., Krajewski, S., Zapata, J. M., Shabaik, A., Gascoyne, R., and Reed, J. C. (1997) *Cancer Res.* **57,** 1605–1613
14. Krajewski, S., Krajewska, M., Ellerby, L. M., Welsch, K., Xie, Z., Deveraux, Q. L., Salvesen, G. S., Bredesen, D. E., Rosenthal, R. E., Fiskum, G., and Reed, J. C. (1999) *Proc. Natl. Acad. Sci. U. S. A.* **96,** 5752–5757
15. Rentrop, M., Knapp, B., Winter, H., and Schweizer, J. (1986) *Histochem. J.* **18,** 271–276
16. Kozak, M. (1992) *Annu. Rev. Cell Biol.* **8,** 197–225
17. Cardone, M., Roy, N., Stennicke, H., Salvesen, G., Franke, T., Stanbridge, E., Frisch, S., and Reed, J. (1998) *Science* **282,** 1318–1321
18. Zhou, P., Chou, J., Olea, R. S., Yuan, J., and Wagner, G. (1999) *Proc. Natl. Acad. Sci. U. S. A.* **96,** 11265–11270
19. Srinivasula, S. M., Ahmad, M., Fernandes-Alnemri, T., and Alnemri, E. S. (1998) *Mol. Cell* **1,** 949–957
20. Li, P., Nijhawan, D., Budihardjo, I., Srinivasula, S., Ahmad, M., Alnemri, E., and Wang, X. (1997) *Cell* **91,** 479–489
21. Thornberry, N., Rano, T., Peterson, E., Rasper, D., Timkey, T., Garcia-Calvo, M., Houtzager, V., Nordstrom, P., Roy, S., Vaillancourt, J., Chapman, K., and Nicholson, D. (1997) *J. Biol. Chem.* **272,** 17907–17911
22. Hu, Y., Benedict, M., Wu, D., Inohara, N., and Nunez, G. (1998) *Proc. Natl. Acad. Sci. U. S. A.* **95,** 4386–4391
23. Green, D. R., and Reed, J. C. (1998) *Science* **281,** 1309–1312
24. Yoshida, H., Kong, Y. Y., Yoshida, R., Elia, A. J., Hakem, A., Hakem, R., Penninger, J. M., and Mak, T. W. (1998) *Cell* **94,** 739–750
25. Kuida, K., Haydar, T. F., Kuan, C.-Y., Gu, Y., Taya, C., Karasuyama, H., Su, M. S.-S., Rakic, P., and Flavell, R. A. (1998) *Cell* **94,** 325–337
26. Haraguchi, M., Torii, S., Matsuzawa, S., Xie, Z., Kitada, S., Yoshida, H., Mak, T. W., and Reed, J. C. (2000) *J. Exp. Med.* **191,** 1709–1720
27. Reed, J. (1999) *J. Clin. Oncol.* **17,** 2941–2953
28. Weinstein, J., Myers, T., O'Connor, P., Friend, S., Fornace, A. J., Kohn, K., Fojo, T., Bates, S., Rubinstein, L., Anderson, N., Buolamwini, J., van Osdol, W., Monks, A., Scudiero, D., Sausville, E., Zaharevitz, D., Bunow, B., Viswanadhan, V., Johnson, G., Wittes, R., and Paull, K. (1997) *Science* **17,** 343–349
29. Nagase, T., Ishikawa, K.-I., Suyama, M., Kikuno, R., Miyajima, N., Tanaka, A., Kotani, H., Nomura, N., and Ohara, O. (1998) *DNA Res.* **5,** 277–286
30. Chu, Z.-L., Pio, F., Xie, Z., Welsh, K., Krajewska, M., Krajewski, S., Godzik, A., and Reed, J. C. (2001) *J. Biol. Chem.* **276,** 9239–9245
31. Hlaing, T., Guo, R.-F., Dilley, K. A., Loussia, J. M., Morrish, T. A., Shi, M. M., Vincenz, C., and Ward, P. A. (2001) *J. Biol. Chem.* **276,** 9230–9238
32. Soengas, M., Alarcon, R., Yoshida, H., Giaccia, A., Hakem, R., Mak, T., and Lowe, S. (1999) *Science* **284,** 156–159